UNCLASSIFIED

AD **272 412**

*Reproduced
by the*

ARMED SERVICES TECHNICAL INFORMATION AGENCY
ARLINGTON HALL STATION
ARLINGTON 12, VIRGINIA

UNCLASSIFIED

U. S. ARMY
TRANSPORTATION RESEARCH COMMAND
FORT EUSTIS, VIRGINIA

TCREC TECHNICAL REPORT 61-138

THE EFFECTS OF AXISYMMETRIC SHEAR ON AIRFOIL CHARACTERISTICS

Task 9R38-11-009-03

Contract DA 44-177-TC-439

December 1961

prepared by :

CORNELL AERONAU'   RATORY, INC.
Buffalo, New Yor¹

DISCLAIMER NOTICE

CORNELL AERONAUTICAL LABORATORY, INC.
OF CORNELL UNIVERSITY
BUFFALO 21, NEW YORK

REPORT NO. AI-1190-A-8

THE EFFECTS OF AXISYMMETRIC SHEAR ON AIRFOIL CHARACTERISTICS

DECEMBER 1961

TASK 9R 38-11-009-03
CONTRACT DA 44-177-TC-439

U.S. ARMY TRANSPORTATION RESEARCH COMMAND
TRANSPORTATION CORPS
FORT EUSTIS, VIRGINIA

BY: _R. J. Sidel_
R. J. Vidal

APPROVED BY: _____
A. Hertzberg, Head
Aerodynamic Research Dept.

James T. Curtis
J. T. Curtis

FOREWORD
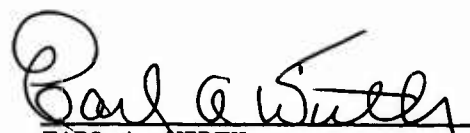
The research on which this report is based was performed by the authors, Mr. R. J. Vidal, Mr. J. H. Hilton, and Dr. J. T. Curtis of the Aerodynamic Research Department of Cornell Aeronautical Laboratory, Inc., Buffalo, New York, under Army Contract DA 44-177-TC-439, Task Number 9R38-11-009-03. The U. S. Army Transportation Research Command, Fort Eustis, Virginia, is the monitoring agency. This work represents a part of a research program, still in progress, which is devoted to investigations of several specific problems associated with STOL/VTOL flight, as well as more general research on the aerodynamics of low-speed flight. This report is one of a series to be published covering the entire program of research.

The report has been reviewed by the U. S. Army Transportation Research Command and is considered technically sound. The report is published for the exchange of information and the stimulation of ideas.

FOR THE COMMANDER:

APPROVED BY:

JAMES G. MC HUGH
USATRECOM Project Engineer

EARL A. WIRTH
CWO-4   USA
Adjutant

TABLE OF CONTENTS

AI-1190-A-8

LIST OF ILLUSTRATIONS

AI-1190-A-8

LIST OF SYMBOLS

L   Lift

D   Drag

m Pitching moment about the midchord station, positive nose up

U   Undisturbed stream velocity at the airfoil position

U_o Reference velocity in a stream with parabolic velocity distribution

ρ Density

c   Airfoil Chord

α Angle of attack

τ Airfoil thickness--chord ratio

y Vertical coordinate measured from airfoil midchord position

k   Local stream shear, $k = \dfrac{c}{U}\dfrac{dU}{dy}$

q Derivative of the stream shear $\dfrac{U}{U_o} = 1 + 8q\left(\dfrac{Y}{c}\right)^2$

C_L Lift coefficient based on local velocity $C_L = \dfrac{L}{\rho/2\ U^2 c}$

C_D Drag coefficient based on local velocity $C_D = \dfrac{D}{\rho/2\ U^2 c}$

C_m Moment coefficient based on local velocity $C_m = \dfrac{M}{\rho/2\ U^2 c^2}$

r   Slipstream radius

AI-1190-A-8

INTRODUCTION

The Cornell Aeronautical Laboratory is conducting a program of theoretical and experimental research on low-speed aerodynamics as applied to STOL and VTOL aircraft. One objective in this research is to study specific aspects of classical aerodynamic information in the light of low-speed flight requirements in order to seek aerodynamic processes which might be exploited to enhance low-speed airplane performance.

A classical problem area that is being examined is that of a propeller slipstream interacting with a wing. In the numerous theoretical treatments of this problem, the first important simplification that is made is to assume a bounded uniform jet superimposed on the main flow field. This is in contrast to the physical situation in which the slipstream has a rotational velocity component, and in which the longitudinal velocity varies markedly with the radius.

In the interests of clarifying one aspect of the wing-propeller slipstream problem, investigations have been made at CAL on the influence of stream shear, or longitudinal velocity gradients, on airfoil characteristics. The approach used in this research is to reduce the problem to its most elementary form for theoretical study, and to extend these results experimentally to a more practical situation. In this way, it is possible to identify clearly the effects of shear in the complex propeller slipstream problem.

The first research was a theoretical treatment of a thick two-dimensional cambered airfoil in an unbounded stream with a linear velocity gradient, i.e., uniform shear.[1] This was followed by an experimental investigation[2,3] to check these theoretical results, and to examine the effects of shear on a two-dimensional airfoil in a bounded two-dimensional slipstream. These experiments

AI-1190-A-8

showed that the onset of airfoil stall occurred at a higher value of lift in a stream with nonuniform shear, which in turn led to a more detailed examination of airfoil stall in a two-dimensional slipstream.[4] Recently, exploratory experiments were made to examine the effects of shear on a two-dimensional airfoil in a simulated axisymmetric slipstream. These experiments closely duplicated the wing-propeller slipstream problem except that rotational velocity components were not present. These were omitted from the experiments, in keeping with the above comments, to isolate the three-dimensional effects of stream shear.

The purpose of this report is to present the data obtained in these recent experiments with a two-dimensional wing in an axisymmetric slipstream. The experimental apparatus is described and the data obtained with the airfoil are presented and compared with theory [1, 3, 5, 6,] and experiment. [4]

TWO-DIMENSIONAL SHEAR EFFECTS ON AIRFOIL CHARACTERISTICS

The completed research on two-dimensional airfoils in shear flows,[2,3,4] together with the existing theory,[1,5,6] shows that there are three major effects of shear on airfoil characteristics. These effects have been discussed in detail in previous reports, and will be briefly reviewed here to serve as a basis for interpreting the experimental data.

Uniform Shear

The theories for two-dimensional airfoils in uniform shear flow[1,6] show there are two effects of shear on airfoil lift. These can be identified by examining the predicted lift for a symmetric airfoil.

$$C_L = \frac{L}{\rho/2\ U^2 c} \approx 2\pi\alpha \left[1 + \tau + \frac{\tau k^2}{32} \right] + \frac{\pi \tau k}{2} \tag{1}$$

U is the undisturbed stream velocity at the airfoil position, and $k = \frac{c}{U}\frac{dU}{dy}$ is the local stream shear. One minor effect of shear is to increase the slope of the lift curve by the factor, $\frac{\tau k^2}{32}$. This factor is normally small in comparison with unity and the increased slope is not of practical importance. The important effect is that the stream shear couples with the airfoil thickness to produce an overall displacement of the lift curve, analogous to that produced by airfoil camber or by a superimposed change in angle of attack. This fact makes it mandatory to study the influence of shear in an idealized slipstream since in an actual propeller slipstream, the rotational velocity components effectively change the local angle of attack. Consequently, the effects of shear cannot be separated from the rotational effects in a simple manner.

3

The magnitude of the lift curve displacement due to stream shear has been theoretically established[1,5] and experimentally verified[3,4] for the two-dimensional case in which the shear flow is unbounded. Shear typical of that in a propeller slipstream can displace the lift curve by $\Delta C_L \approx 0.6$. In two-dimensional bounded shear flow, this displacement due to shear is about 50% of that in the unbounded case. The remaining question to be answered, in regard to axisymmetric slipstreams, concerns the three-dimensional effect on the lift increment due to shear.

Nonuniform Shear

There are three important effects of nonuniform shear on symmetrical airfoil characteristics. The first of these, which has been theoretically predicted,[6] is a change in lift curve slope proportional to the derivative of the local stream shear.

$$C_L = \frac{L}{\rho/2 \; U^2 c} \approx 2\pi\alpha \left[1 + \tau - q \left(0.8841 + \ln q \right) \right]$$ (2)

The parameter, q, is essentially the derivative of the stream shear, $U = U_o \left[1 + 8q \left(\frac{Y}{c} \right)^2 \right]$. Equation (2) applies only for small values of q, and for $q = 1/4$ predicts a 20% increase in lift curve slope. This effect of shear derivative has been qualitatively verified in experiments simulating a two-dimensional propeller slipstream.[3] The experimental flow corresponded to $q \approx 2$, and the observed increase in lift curve slope was 250%.

The second effect of nonuniform shear on airfoil characteristics stems from the coupling of the airfoil thickness with the stream shear to produce a displacement of the lift curve. It has been demonstrated theoretically and

AI-1190-A-8

experimentally verified [4] that this effect is the same as that observed in uniform shear. In addition, a typical effect of the slipstream boundary is to diminish the lift increment due to shear by about 50%.

A third effect of nonuniform shear is to change the airfoil maximum lift. This effect has been demonstrated experimentally,[4] but a theoretical explanation of the effect is lacking. The experimental data suggest that in nonuniform shear flow, the airfoil maximum lift is determined by the product of the local shear and the local derivative of the shear. Stall is delayed if this product is negative, promoted if the product is positive, and stall is unaffected if the product is zero. These results were obtained under two-dimensional conditions; the three-dimensional shear effect on airfoil stall is examined here.

AI-1190-A-8

EXPERIMENTAL APPARATUS

The experiments were made in the subsonic leg [7] of the CAL One-Foot High Speed Wind Tunnel. [8] This leg of the wind tunnel has a test section with a cross-section of 17" by 24", and is operated as a closed throat non-return type tunnel. The test section stagnation pressure is one atmosphere and the speed range is from 0 to 100 fps.

The shear in the test flow was generated by a nonuniform screen placed across the wind tunnel test section upstream of the model. In effect, the screen is an inverse propeller in that it removes energy from the external free stream, and redistributes the energy within the slipstream by selectively introducing losses. The chief advantage of this technique is that it provides a basis for the systematic study of slipstream flow nonuniformities, in that the various characteristics of a slipstream flow can be controlled and introduced at will. This technique can also be used to study slipstream effects under two-dimensional conditions.

Shear Screens

In designing a screen to produce a desired shear flow, it must be noted that the static pressure immediately downstream of the screen is not constant over the screen because the screen losses are not uniform. Far downstream the flow readjusts to a condition of uniform static pressure. Consequently, it is not possible to simply extrapolate the desired velocity distribution back to the screen to determine the required distribution of screen losses.

Owen and Zienkiewicz [9] have presented a method for designing screens to produce a uniform shear. That method is restricted to two-dimensional flows

AI-1190-A-8

with a linear velocity distribution and to screens which only slightly perturb the flow. Since here the research is concerned with large nonuniform and discontinuous shear, it was necessary to extend the screen theory to include these cases for both two-dimensional and axisymmetric flows. The two-dimensional theory is reported in Ref. 3. The theory for axisymmetric screens is given in the Appendix.

Briefly, the theory for nonuniform screens is based on a duct flow and postulates disturbance stream functions associated with the screen which vanish far upstream of the screen, and reduce to the desired velocity distribution far downstream of the screen. Further, these disturbance stream functions differ on either side of the screen but are equal at the screen. It is required that the longitudinal velocity be continuous through the screen, and that the vertical velocity change through the screen by a factor related to the screen resistance. These conditions then fix the screen disturbance stream function as a function of the desired velocity distribution. The requirement that the static pressure be uniform across the flow at large distances for the screen, plus the assumption that the total pressure loss on any streamline is the local screen loss then relate the desired velocity distribution to the distribution of screen resistance.

The methods used in designing and fabricating two-dimensional screens[3] were applied in fabricating the axisymmetric screen. In order to have a direct experimental check of shear effects on an airfoil, the axisymmetric screen was designed to duplicate the design parameters used in the two-dimensional research.[3] That is, the screen was designed to produce a linear velocity distribution in the slipstream with a shear defined by $k = 2$. Further, the average velocity in the slipstream was to be about twice that in the external flow.

AI-1190-A-8

The screen, Figure 1, was constructed of high-solidity uniform screen to produce the uniform external stream. The nonuniform portion, producing the 6-inch diameter axisymmetric shear flow, consisted of 1/8" diameter rods bent into concentric circles and suitably spaced to give the desired solidity. The entire screen assembly was bonded to a metal honeycomb and mounted in a metal frame. The honeycomb served to stiffen the assembly structurally and to prevent flow instabilities.[3] It will be noted that the screen producing the external flow was uniform, though the screen theory called for a solidity distribution that varied by about 3% over the external flow. It was decided to simplify the fabrication by using a uniform screen since the resulting nonuniformities would not be important.

Previous experiments with two-dimensional screens[2,3] showed that excessive mixing occurred between the simulated slipstream and the external flow if the slipstream was not physically separated by plates from the external flow. For this reason, the axisymmetric slipstream was constrained in a constant-area duct to a point about one slipstream diameter ahead of the airfoil. The screen-duct arrangement is shown in Figure 2.

The screen was positioned one slipstream radius from the centerline of the wind tunnel. This off-center location was used so that airfoil section loads could be measured on the wing well outside the jet boundary. The flow produced by the screen was calibrated to determine the velocity distribution and the flow angularity using a conventional 1/8" diameter pitch-yaw pitot-static probe. The velocity data were not corrected for the shear flow displacement effect[10] since in this instance the effect on velocity was negligibly small. This displacement effect influenced the indicated flow angularity, since it is manifested as a

AI-1190-A-8

distorted pressure distribution. The flow angularity measurements were corrected using the available theory [10] and the corrected angularity was less than 1/2° at all locations surveyed.

The distributions of velocity produced by the screen are shown in Figure 3. Figure 3a is a plot of constant velocity contours derived from surveys at the three stations indicated. These data show that the tunnel wall proximity caused a small displacement of the jet towards the wall. It seems likely that the wall would also distort the jet, though no distortion is evident in the data. The velocity data obtained at each of the three survey stations are compared with the theoretical predictions in Figures 3b - 3d. The data agree reasonably well with the theory inside the jet, but the velocities outside the jet are somewhat higher than predicted. This discrepancy probably can be ascribed to a small error in screen solidity. The portions of the screen producing this external flow had a solidity of about 60%. A 10% error in solidity would account for the observed discrepancies. The data from survey station C show appreciable velocity deviations. These apparently stem from local changes in solidity.

The distributions of shear in the jet were determined from the velocity calibration data, and are plotted in Figure 4. As noted earlier, the screen was designed to produce a uniform shear flow, $k = 2$, and the data show the shear was approximately uniform at survey stations A and B. The data from station C show marked changes in shear because of the local variations in screen solidity.

Airfoil Model

The airfoil used in this research was an uncambered two-dimensional Joukowsky airfoil with a thickness-chord ratio of 17% and a chord of six inches.

AI-1190-A-8

A two-dimensional airfoil was selected for the experiments because of the analytic and experimental simplicity. The three-dimensional effect that would be present would be from the spanwise variation in shear and from the wing vorticity shed in the vicinity of the slipstream. The analytic complications associated with a tip and the associated nonuniform loading would not be present, thereby simplifying the interpretation of the results.

The model, shown in Figure 5, was instrumented with a three-component internal strain gauge balance to measure the loads on one section of the airfoil. This instrumented section had an aspect ratio of 0.125. The remainder of the airfoil was similarly segmented so that the instrumented section could be positioned at any spanwise station. The model was assembled with gaps on either side of the instrumented section to prevent balance interference. The entire model was then wrapped with 0.005" thick sheet rubber to prevent flow through the gaps, and the balance was calibrated with the sheet rubber in place. The balance was designed to measure a maximum lift of about three pounds. During the calibration it was demonstrated that the entire system, including the rubber sheet, was linear to better than 1/2%, and that by including these nonlinearities in the calibration, the balance would resolve a lift force of about 0.01 pounds.

AI-1190-A-8

RESULTS

The intent in this research is to survey completely the load distribution with the airfoil positioned at various locations in the nonuniform slipstream. The present exploratory experiments were made to define areas for more detailed investigations. The limited data that were acquired qualitatively illustrate the influence of shear in axisymmetric stream.

Shear Effects on Section Characteristics

The experiments consisted of measuring the section lift, drag, and pitching moment at one spanwise station in the slipstream with the airfoil positioned at two vertical locations in the slipstream. The spanwise measurement station was approximately 0.08 slipstream diameter from the slipstream centerline (Survey Station A in Figure 3). The measurements were made with the airfoil positioned at $y/r = -1/16$ and $y/r = +1/2$. The results are plotted in Figures 6, 7, and 8.

The lift data (Figure 6) are compared with the two-dimensional theory to assess the three-dimensional shear effects. Noting the shear distribution in Figure 4, the data obtained at $y/r = -1/16$ are compared with the nonuniform shear theory,[6] corrected for two-dimensional boundary interference.[3] Those obtained at $y/r = +1/2$ are compared with the uniform shear theory,[1] corrected for two-dimensional boundary interference.

Considering the data for $y/r = -1/16$, it can be seen that the agreement between theory and experiment is very good. The lift curve slope is accurately predicted, and the only important discrepancy stems from inaccuracies

11   AI-1190-A-8

in predicting the displacement of the lift curve due to shear. The theory, uncorrected for boundary interference, predicts a displacement due to shear of $\Delta C_L = -0.27$; the experiment shows $\Delta C_L = .05$. Application of the boundary correction to the two-dimensional theory accounts for about 77% of the difference between these two values. This boundary correction has proved accurate in previous two-dimensional research.[2,4] It appears that the small discrepancy between theory and experiment stems from three-dimensional changes in the boundary correction.

The two-dimensional theory, corrected for two-dimensional boundary interference, is compared with the lift data obtained at $y/r = +1/2$ in Figure 6. It can be seen again that the theory predicts the lift curve slope with reasonable accuracy. However, the predicted displacement of the lift curve due to shear is markedly different from the experimental value. The uncorrected two-dimensional theory predicts $\Delta C_L = .45$. The two-dimensional boundary correction accounts for about 50% of the change in lift increment due to shear. It appears that difference between theory and experiment again stems from three-dimensional boundary interference effects.

The pitching moment data are compared with the appropriate two-dimensional theory in Figure 7. The comparison shows that the theory predicts the center of pressure position with reasonable accuracy. However, the theory is inadequate for estimating the pitching moment at zero lift. The theory for pitching moment exhibits some inaccuracies in the two-dimensional case, and the observed discrepancies cannot be attributed entirely to three-dimensional effects.

AI-1190-A-8

The section drag data for the airfoil in the axisymmetric slipstream are presented in Figure 8. It will be noted that in the vicinity of zero lift, the drag is less than the laminar skin friction ($C_D \approx .01$). This effect was observed in previous research,[3] and stems from the artificially high level of turbulence induced by the shear screens. The effect of the turbulence is to artificially thicken the boundary layer on the airfoil, thereby decreasing the boundary layer shear and the skin friction.

Shear Effects on Maximum Lift

The lift data in Figure 6 show that with the airfoil positioned at $y/r = -1/16$ stall was imminent at the highest angles of attack. However, the lift data for $y/r = 1/2$ show no clear break in the lift curve, though the behavior suggests an approach to stall. The drag data, Figure 8, indicate stall at the highest angles of attack in both cases, and it is concluded that stall was imminent in both cases.

Previous two-dimensional experiments [4] have shown that stream shear can markedly alter airfoil maximum lift. One purpose of the present experiments was to examine the influence of axisymmetric shear on maximum lift. The maximum lift shown in Figure 6 has been reduced to coefficient form using the average slipstream velocity and corrected for boundary interference effects for comparison with the two-dimensional results. This comparison is made in Figure 9. These preliminary data show that higher maximum lifts are obtained in the axisymmetric slipstream, and that the maximum lift is apparently independent of the stream shear. This is in contrast to the two-dimensional results which show that maximum lift varies markedly with the local stream shear and its derivative.

13

AI-1190-A-8

CONCLUDING REMARKS

The preliminary data presented for an airfoil in a stream with axisymmetric shear demonstrate that the two-dimensional analysis can be applied to three-dimensional problems in certain instances. In particular, the present results suggest that near the center of the slipstream, the two-dimensional data, corrected for two-dimensional boundary interference, can be used in a strip analysis to predict the slope of the lift and moment curves.

The two-dimensional approach cannot be used to predict the displacement of the lift curve due to shear, evidently because the boundary interference is not accurately included. It is demonstrated in Ref. 4 that the changes in the lift increment due to shear stem from "thickness" interference with the slipstream boundary. That is, if the airfoil thickness is a significant fraction of the slip-stream height, the boundary will be distorted and will produce additional disturbance velocities on the airfoil. These disturbance velocities reduce the displacement of the lift curve. The two-dimensional theory [3] includes approximate corrections for thickness effects. However, the present data suggest that a more refined thickness model is required.

The two-dimensional research[4] showed that stream shear could markedly influence airfoil stall, and it was concluded on the basis of the experimental data, that the governing parameter was the product of the local shear and its derivative. The two maximum lift data points obtained in the present investigation show that the maximum lift is greater in axisymmetric slipstreams than in the two-dimensional case. In addition, these data suggest that the maximum lift is essentially independent of the stream shear in an axisymmetric slipstream.

14   AI-1190-A-8

No firm conclusion can be reached on this effect because of the limited information, and further research is required to clarify this point.

AI-1190-A-8

APPENDIX

THE PRODUCTION OF A SPECIFIED AXISYMMETRIC
SHEAR FLOW BY A NONUNIFORM STREAM

In order to determine the aerodynamic characteristics of airfoils in a simulated propeller slipstream free of rotational velocity components, it is necessary to product a specified nonuniform flow with large velocity gradients. As originally demonstrated [9] and subsequently extended, [3] this can be accomplished using screens with the proper distribution of resistance mounted upstream of the test region. The cited methods are restricted to two-dimensional flows. The present work is an extension of the theory of Ref. 3 to include screen producing axisymmetric flows.

The model used is an initially uniform constant area channel flow (Station 0 in Figure 10) which subsequently passes through a nonuniform screen, Stations 1 and 2, and expands to its final configuration far downstream at Station 3. Stations 1 and 2 refer to the upstream side and the downstream side of the screen, respectively. Using the nomenclature shown in Figure 10, the final velocity distribution at Station 3 can be considered to be the uniform stream velocity with a perturbation velocity added.

$$U_3(R) = U_0 + w(R)$$

Introducing the dimensionless coordinates, $\xi = \dfrac{x}{H/2}$, $\eta = \dfrac{R}{H/2}$ a stream function is defined such that

$$u = \frac{U}{U_0} = \frac{1}{\eta} \frac{\partial \psi}{\partial \eta} \qquad\qquad v = \frac{V}{U_0} = -\frac{1}{\eta} \frac{\partial \psi}{\partial \xi} \tag{I-1}$$

AI-1190-A-8

The boundary conditions to be satisfied are

(1) The longitudinal velocity component is continuous through the screen.

$$\left(\frac{\partial \psi}{\partial \eta}\right)_{\xi=-0} = \left(\frac{\partial \psi}{\partial \eta}\right)_{\xi=+0} \tag{I-2}$$

(2) The transverse velocity component changes by a factor, β, through the screen.

$$\left(\frac{\partial \psi}{\partial \xi}\right)_{\xi=-0} = \frac{1}{\beta}\left(\frac{\partial \psi}{\partial \xi}\right)_{\xi=+0} \tag{I-3}$$

(3) The transverse velocity is zero at the channel wall.

$$-\left(\frac{\partial \psi}{\partial \xi}\right)_{\eta=1} = 0 \tag{I-4}$$

(4) The transverse velocity component is non-zero and finite at the center of the channel.

$$\left(\frac{1}{\eta}\frac{\partial \psi}{\partial \eta}\right)_{\eta=0} \equiv finite \neq 0 \tag{I-5}$$

Introducing a disturbance stream function, ψ_1, such that

$$\xi < 0 \qquad \psi = \frac{1}{2}\eta^2 + \psi_1 \tag{I-6}$$

$$\xi > 0 \qquad \psi = \frac{1}{2}\eta^2 + \psi_1 + \int_0^\eta \eta\, w(\eta)\, d\eta \tag{I-7}$$

The disturbance stream function must then satisfy the condition

$$\frac{\partial^2 \psi_1}{\partial \eta^2} - \frac{1}{\eta}\frac{\partial \psi_1}{\partial \eta} + \frac{\partial^2 \psi_1}{\partial \eta^2} = 0 \tag{I-8}$$

The general solution may be obtained by separating variables.

AI-1190-A-8

$$\xi < 0 \qquad \psi_1 = \sum_{n=1}^{\infty} A_n \eta \, J_1(\lambda_n \eta) \, e^{\lambda_n \xi}$$

$$\xi > 0 \qquad \psi_1 = \sum_{n=1}^{\infty} C_n \eta \, J_1(\lambda_n \eta) \, e^{-\lambda_n \xi} \tag{I-9}$$

The second solution $N_1(\lambda_n \eta)$ becomes infinite at the origin and so is excluded.

The velocity at the wall is zero, Eq. (I-4)

$$\xi < 0 \qquad v = -\frac{1}{\eta} \frac{\partial \psi_1}{\partial \xi} = -\sum_{n=1}^{\infty} A_n \lambda_n \, J_1(\lambda_n) \, e^{\lambda_n \xi}$$

$$\xi > 0 \qquad v = -\frac{1}{\eta} \frac{\partial \psi_1}{\partial \xi} = \sum_{n=1}^{\infty} C_n \lambda_n \, J_1(\lambda_n) \, e^{-\lambda_n \xi}$$

so that

$$J_1(\lambda_n) = 0 \; .$$

Let

$$\int_0^{\eta} t \, w(t) \, dt \equiv \eta \, f(\eta) \tag{I-10}$$

and assume

$$f(\eta) = \sum_{n=1}^{\infty} D_n \, J_1(\lambda_n \, \eta) \tag{I-11}$$

where

$$D_n = \frac{2}{J_2^2(\lambda_n)} \int_0^1 t \, f(t) \, J_1(\lambda_n, t) \, dt \; . \tag{I-12}$$

Then, in general

$$\xi < 0 \qquad v = \sum_{n=1}^{\infty} A_n \lambda_n \, J_1(\lambda_n \eta) \, e^{\lambda_n \xi}$$

$$\xi > 0 \qquad v = \sum_{n=1}^{\infty} C_n \lambda_n \, J_1(\lambda_n \eta) \, e^{-\lambda_n \xi}$$

18   AI-1190-A-8

and

$$\xi < 0 \qquad u = \frac{1}{\eta} \frac{\partial \psi}{\partial \eta} = \sum_{n=1}^{\infty} A_n \lambda_n J_o(\lambda_n \eta) e^{\lambda_n \xi} + 1$$

$$\xi > 0 \qquad u = 1 + \sum_{n=1}^{\infty} C_n \lambda_n J_o(\lambda_n \eta) e^{-\lambda_n \xi} + \sum_{n=1}^{\infty} D_n \lambda_n J_o(\lambda_n \eta)$$

Applying the boundary conditions given in Eq. (I-2) and (I-3),

$$A_n = C_n + D_n$$

whence

$$A_n = -\frac{1}{\beta} C_n$$

$$A_n = \frac{D_n}{1+\beta} \tag{I-13}$$

$$C_n = -\frac{\beta}{1+\beta} D_n \tag{I-14}$$

The condition for a single streamtube is

$$\psi(0, \eta_2) = \psi(\infty, \eta_3)$$

or

$$\frac{1}{2} \eta_2^2 + \sum_{n=1}^{\infty} C_n \eta_2 J_1 + \eta_2 f(\eta_2) = \eta_3 f(\eta_3) + \frac{1}{2} \eta_3^2 \quad .$$

From Eq. (I-14)

$$\frac{1}{2} \eta_2^2 - \frac{\beta}{1+\beta} \sum_{n=1}^{\infty} D_n \eta_2 J_1 + \eta_2 f(\eta_2) = \eta_3 f(\eta_3) + \frac{1}{2} \eta_3^2$$

and from Eq. (I-11)

$$\frac{1}{2} \eta_2^2 - \frac{\beta}{1+\beta} \eta_2 f(\eta_2) + \eta_2 f(\eta_2) = \eta_3 f(\eta_3) + \frac{1}{2} \eta_3^2 \quad .$$

Combining these relations leads to the following relation for the streamtube coordinates

$$\frac{1}{2} \eta_2^2 + \frac{1}{1+\beta} \eta_2 f(\eta_2) = \eta_3 f(\eta_3) + \frac{1}{2} \eta_3^2 \quad . \tag{I-15}$$

In order to proceed further, it is now necessary to relate the total pressure along any streamline to the local screen resistance on that streamline. As in the previous development,[3] it is assumed that on any streamline, the change in total pressure is the local screen resistance. That is $\frac{p_1 - p_2}{\rho/2\ U_0^2} = K\left(\frac{U_1^2 + V_1^2}{U_0^2}\right)$. In addition, an average screen resistance is defined as

$$\overline{K} = \frac{p_0 - p_3}{\rho/2\ U_0^2} \quad .$$

By stipulating that the total pressure is conserved upstream of the screen and downstream of the screen, it is then possible to relate the local screen resistance to the final distribution of velocities. This development parallels that given in Ref. 3, and will not be repeated. Assuming that Taylor and Batchelor's refraction coefficient [11] for uniform screens applies locally for nonuniform screens, the factor, β , in Eq. (I-3) is then given by

$$\beta = \frac{1.1}{\sqrt{1+K}}$$

The final relation for the total pressure defect along any streamline is

$$\left[-F^2 + \gamma_3^2 - \overline{K} - 2\right]\beta^4 - 2\left[\overline{K} + 1 + \gamma_2 - \gamma_3^2\right]\beta^3 + \left[0.21 - \gamma_2^2 + \gamma_3^2 - \overline{K}\right]\beta^2$$

$$+ 2.42\ \gamma_2\ \beta + 1.21\left[F^2 + \gamma_2^2\right] = 0 \tag{I-16}$$

where $\quad \gamma_2 = \dfrac{U_2(R)}{U_0} = 1 + \dfrac{w_2(R)}{U_0}\ , \quad \gamma_3 = \dfrac{U_3(R)}{U_0} = 1 + \dfrac{w_3(R)}{U_0}$

AI-1190-A-8

and the quantity, F , is defined as

$$F = -\sum_{n=1}^{\infty} D_n \lambda_n \, J_1 (\lambda_n , \eta_2) \cdot \tag{I-17}$$

The problem is solved, in principal, by Eq. (I-16) in combination with Equations (I-12), (I-15), and (I-17). The application of these results can be tedious, and the mathematical techniques employed in the design of the screen in Figure 1 will be summarized. The screen design called for a linear distribution of velocity within the simulated slipstream, and a uniform exterior stream. In addition, the slipstream diameter was to be one third of the channel diameter. That is,

$$0 \leq \eta \leq \tfrac{1}{3} \qquad w(\eta) = a + b\eta \qquad f(\eta) = \frac{1}{\eta} \int_0^{\eta} t\, w(t)\, dt = \frac{a}{2} \eta + \frac{b}{3} \eta^2$$

$$\tfrac{1}{3} < \eta \leq 1 \qquad w(\eta) = 1 \qquad f(\eta) = \frac{1}{\eta} \int_0^{\eta} t\, w(t)\, dt = \frac{a}{2} \eta + \frac{b}{81\eta} \cdot \tag{I-18}$$

The coefficients, D_n , can be evaluated from Eq. (I-12) using the reduction formulas given by Watson [12](pg. 133). After repeated application of these formulae, the coefficients can be expressed as

$$D_n = \frac{2}{J_2^2(\lambda_n)} \left\{ \frac{a}{2} \frac{J_2(\lambda_n)}{\lambda_n} - \frac{b}{81\lambda_n} \left[J_0(\lambda_n) - J_0\!\left(\frac{\lambda_n}{3}\right) \right] + \frac{b}{3} \left[\frac{1}{27\lambda_n} J_2\!\left(\frac{\lambda_n}{3}\right) \right.\right.$$
$$\left.\left. + \frac{1}{9\lambda_n^2} J_1\!\left(\frac{\lambda_n}{3}\right) \right] - \frac{b}{\lambda_n^4} \left[\frac{\lambda_n}{3} J_2\!\left(\frac{\lambda_n}{3}\right) - J_1\!\left(\frac{\lambda_n}{3}\right) + \int_0^{\frac{\lambda_n}{3}} \frac{J_1(z)}{z}\, dz \right] \right\} \cdot \tag{I-19}$$

The integral in Eq. (I-19) is tabulated to high values of the argument in Ref. 13.

In passing, it should be noted that the series expression for $f(\eta)$, Eq. (I-11) converges for $\eta \neq 0$ and $\eta \neq 1$ since $\int_0^1 \sqrt{\eta} \, f(\eta)\, d\eta$ exists and is

AI-1190-A-8

uniformly convergent and $f(t)$ has limited total fluctuations in this interval. The convergence is uniform since f is continuous (see Ref. 12, pg. 591).

The next step is to evaluate Eq. (I-15) to determine the edge of the nonuniform stream at the screen. Taking $\eta_3 = 1/3$ and $\eta_2 = \varepsilon$, and assuming $\varepsilon < 1/3$, $\beta = 1$, Eq. (I-15) yields a contradiction, $\varepsilon = 0.376 > 1/3$. Therefore $\varepsilon > 1/3$. Solving Eq. (I-15) subject to this restriction yields

$$\varepsilon = \frac{1}{3}\left(\frac{1+a+b/9}{1+a/2}\right)^{1/2} \quad .$$

The streamtube equations then become

For $\quad 0 \leq \eta_2 \leq \frac{1}{3}$, $\quad 0 \leq \eta_3 \leq \frac{1}{3}$ $\qquad\qquad$ (I-20)

$$\frac{2b}{3}\eta_3^2 + (1+a)\eta_3^2 - \frac{2b}{3(1+\beta)}\eta_2^3 - \eta_2^2\left(1+\frac{a}{1+\beta}\right) = 0 \ .$$

For $\quad \frac{1}{3} < \eta_2 \leq \varepsilon$, $\quad 0 \leq \eta_3 \leq \frac{1}{3}$ $\qquad\qquad$ (I-21)

$$\frac{2b}{3}\eta_3^3 + (1+a)\eta_3^2 - \left(1+\frac{a}{1+\beta}\right)\eta_2^2 + \frac{a}{1+\beta} = 0 \ .$$

For $\quad \varepsilon < \eta_2 < 1$, $\quad \frac{1}{3} < \eta_3 < 1$ $\qquad\qquad$ (I-22)

$$\eta_2^2\left(1+\frac{a}{1+\beta}\right) - \frac{a}{1+\beta} - \eta_3^2(1+a) + a = 0 \ .$$

To determine the screen resistance for $\eta_2 < \varepsilon$, it is necessary to solve the resistance equation, Eq. (I-16), and Eq. (I-20) or (I-21) simultaneously. The simplest procedure is to solve the resistance equation for γ_3 and then express η_3 in terms of γ_3 by the appropriate formula. Using the resulting

AI-1190-A-8

equation, it is possible to plot η_3 as a function of β for a fixed η_2. Equation (I-20) or (I-21) can also be solved for β for a fixed value of η_2 and varying η_3. This yields a second graphical solution for η_3 as a function of β, and the intersection of the two curves yields the solution.

This procedure is unnecessary for $\eta_2 > \varepsilon$ since γ_2 and γ_3 are both independent of η. In this case the resistance equation can be solved directly for β.

AI-1190-A-8

REFERENCES

1. Sowyrda, A., Theory of Cambered Joukowsky Airfoils in Shear Flow. CAL Report No. AI-1190-A-2, September 1958.

2. Vidal, R. J., Sowyrda, A., and Hartunian, R. A., The Aerodynamic Appraisal of STOL/VTOL Configurations. CAL Report No. AI-1190-A-4, June 1960.

3. Vidal, R. J., Hilton, J. H., and Curtis, J. T., The Two-Dimensional Effects of Slipstream Shear on Airfoil Characteristics. CAL Report No. AI-1190-A-5, TREC TR 60-56, September 1960.

4. Vidal, R. J., Curtis, J. T., and Hilton, J. H., The Influence of Two-Dimensional Stream Shear on Airfoil Maximum Lift. CAL Report No. AI-1190-A-7, TCREC TR 61-93, August 1961.

5. Tsien, H. S., Symmetric Joukowsky Airfoils in Shear Flow. Quart. Appl. Math. Vol. 1, pp. 130-148, 1943.

6. Jones, E. E., The Forces on a Thin Airfoil in Slightly Parabolic Shear Flow. Z. Angew., Math. Mech., Vol. 37, pp. 362-370, 1957.

7. Vidal, R. J., Research on Rotating Stall in Axial Flow Compressors, Part III. Experiments on Laminar Separation from a Moving Wall. CAL Report No. AM-1076-A-3 (WADC TR 59-75, Part III), January 1959.

8. Wilder, J. G., Hindersinn, K., and Weatherston, R., Design of an Air Supply System and Test Section for Research on Scavenging Systems for Propulsion Wind Tunnels. CAL Report No. AD-761-A-1 (WADC TR 56-6), December 1955.

9. Owen, P. R., and Zienkiewicz, H. K., The Production of Uniform Shear Flow in a Wind Tunnel. Jour. Fluid Mech., Vol. 2, Part 6, pp. 521-531, August 1957.

10. Hall, I. M., The Displacement Effect of a Sphere in a Two-Dimensional Shear Flow. Jour. Fluid Mech., Vol. 1, Part 2, pp. 129-141, July 1956.

11. Taylor, G. I., and Batchelor, G. K., The Effect of Wire Gauze on Small Disturbances in a Uniform Stream. Quart. Jour. Mech. Appl. Math., Vol. II, Part 1, pp. 1-29, 1949.

12. Watson, G. N., A Treatise on the Theory of Bessel Functions, 2nd Edition. The MacMillan Co., 1945.

13. Gans, R., Mikroskopiche Probleme. Ann. Physik, Vol. 78, No. 4, p. 22, 1925.
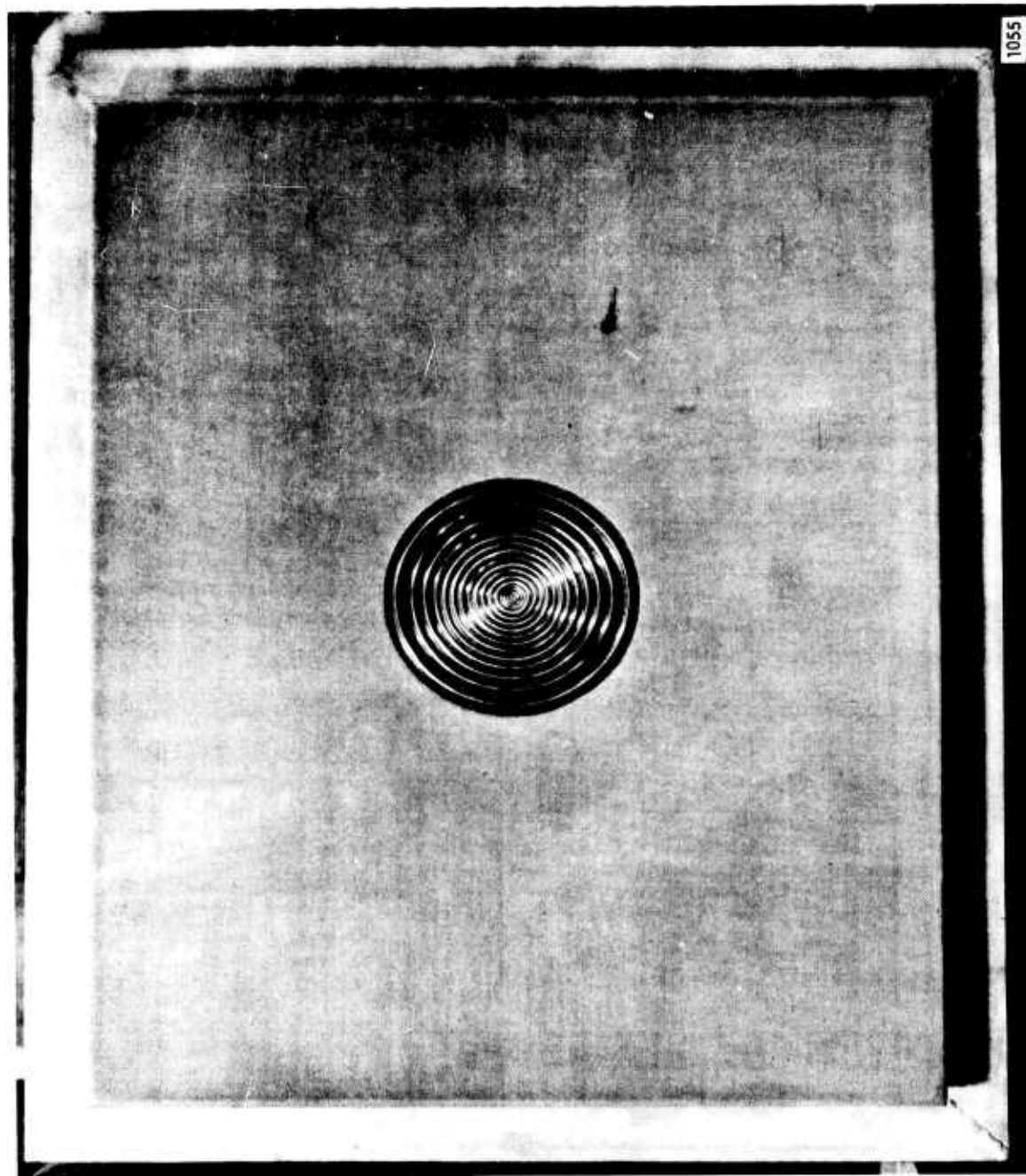
Figure I   UPSTREAM VIEW OF AXISYMMETRIC SHEAR SCREEN

1055
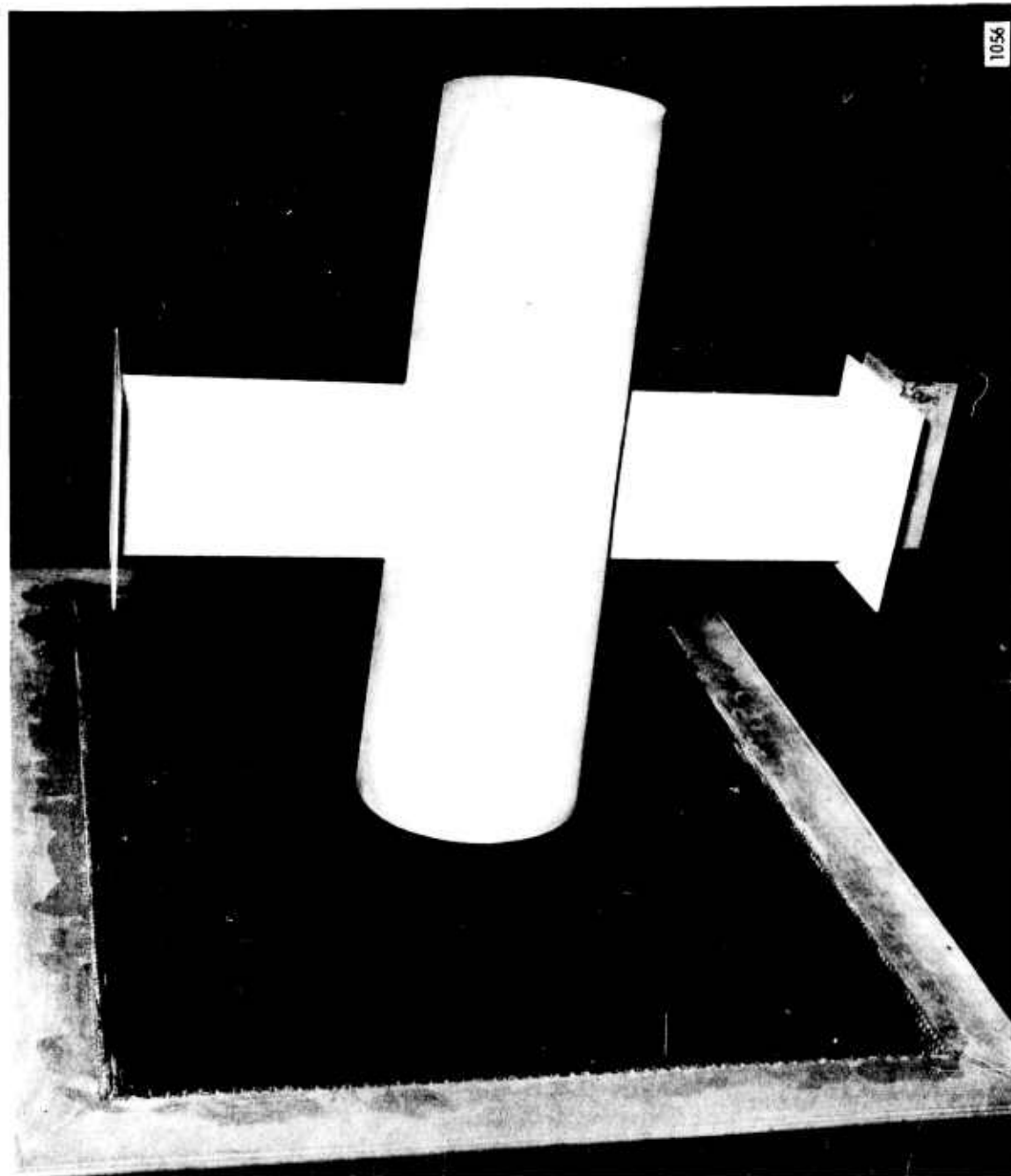
Figure 2 DOWNSTREAM VIEW OF AXISYMMETRIC SHEAR SCREEN WITH DUCT

1056
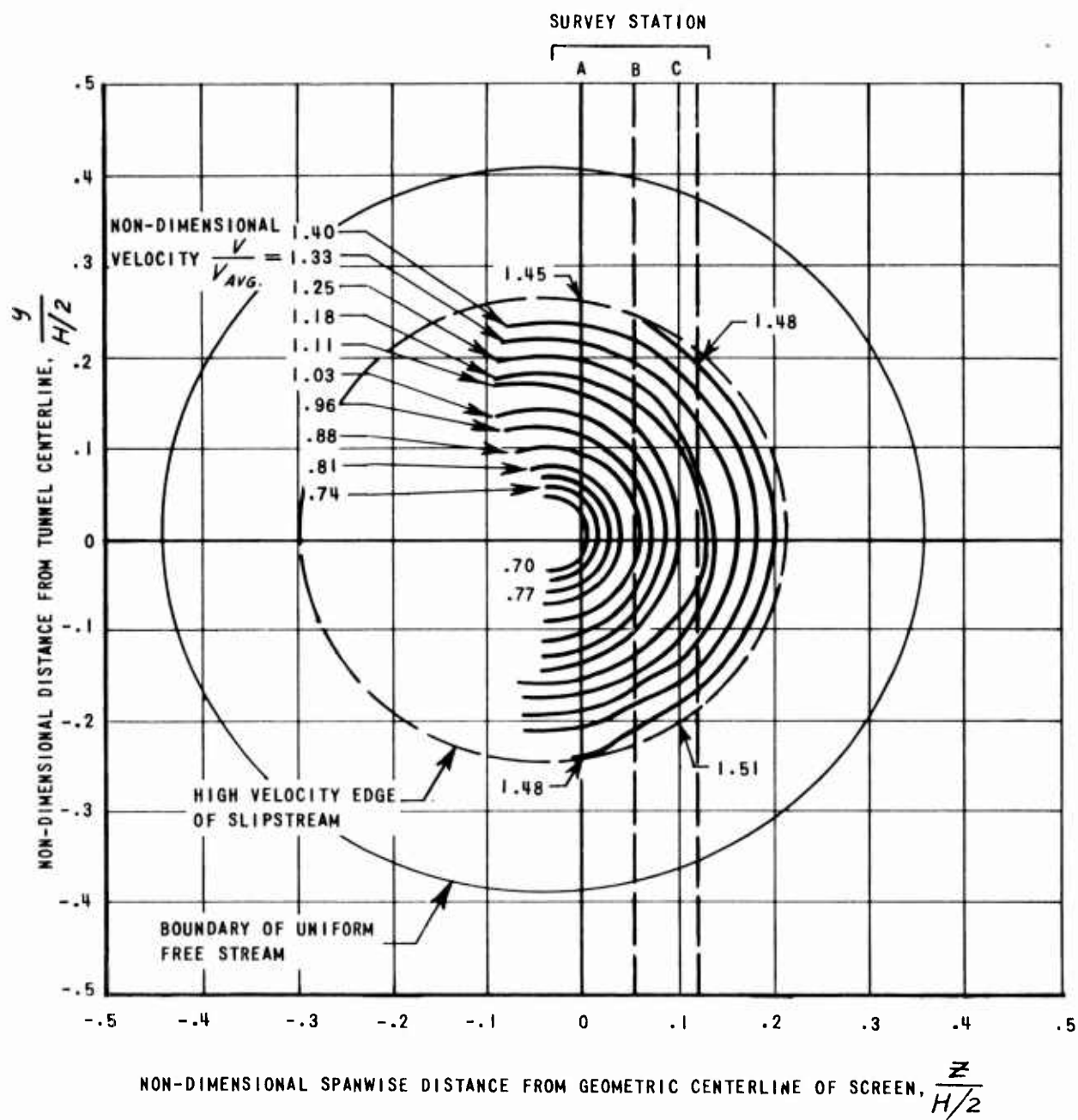
Figure 3a   VELOCITY DISTRIBUTION IN THE AXISYMMETRIC
SLIPSTREAM

27
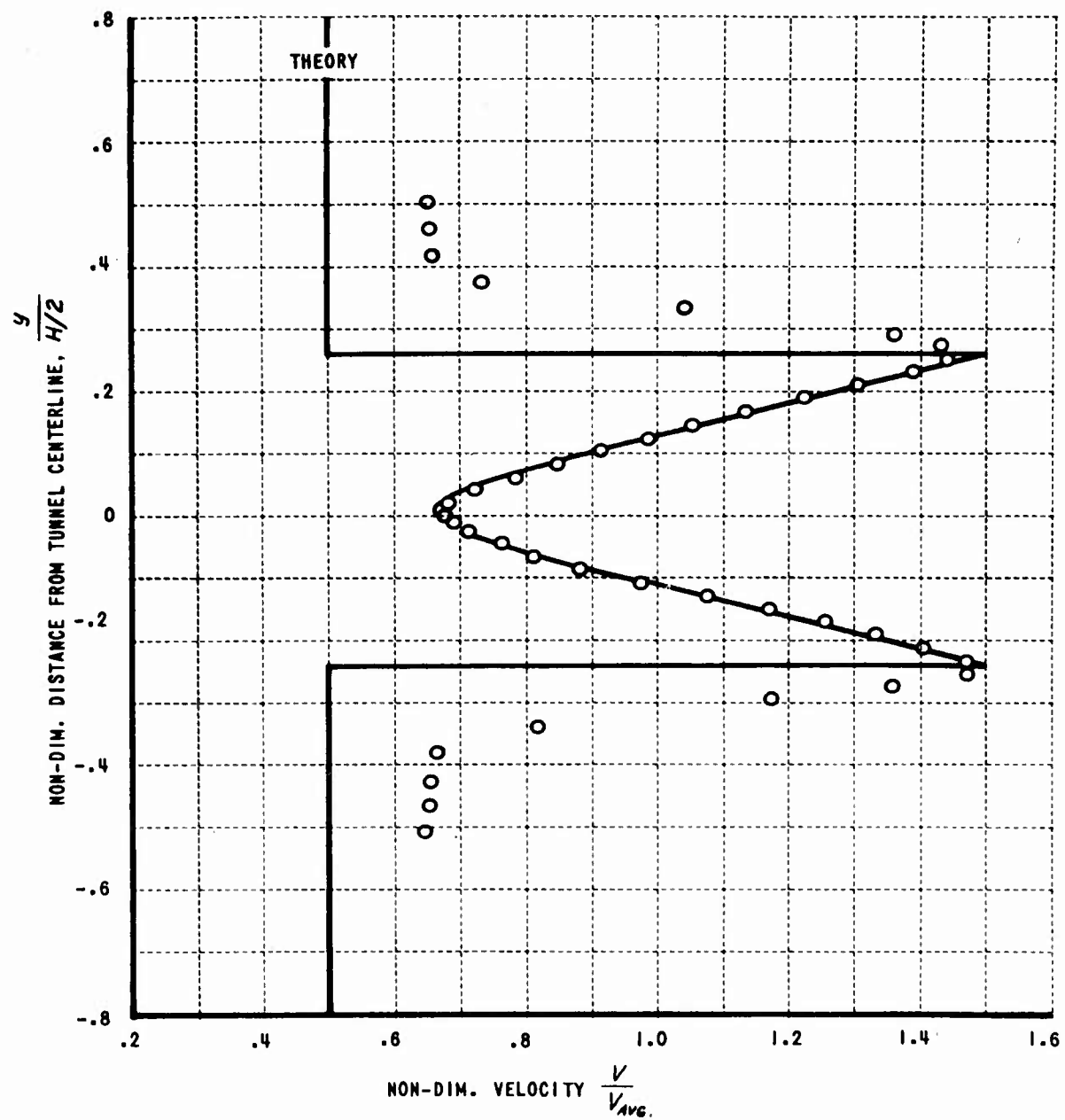
Figure 3B   VELOCITY DISTRIBUTION - STA.A
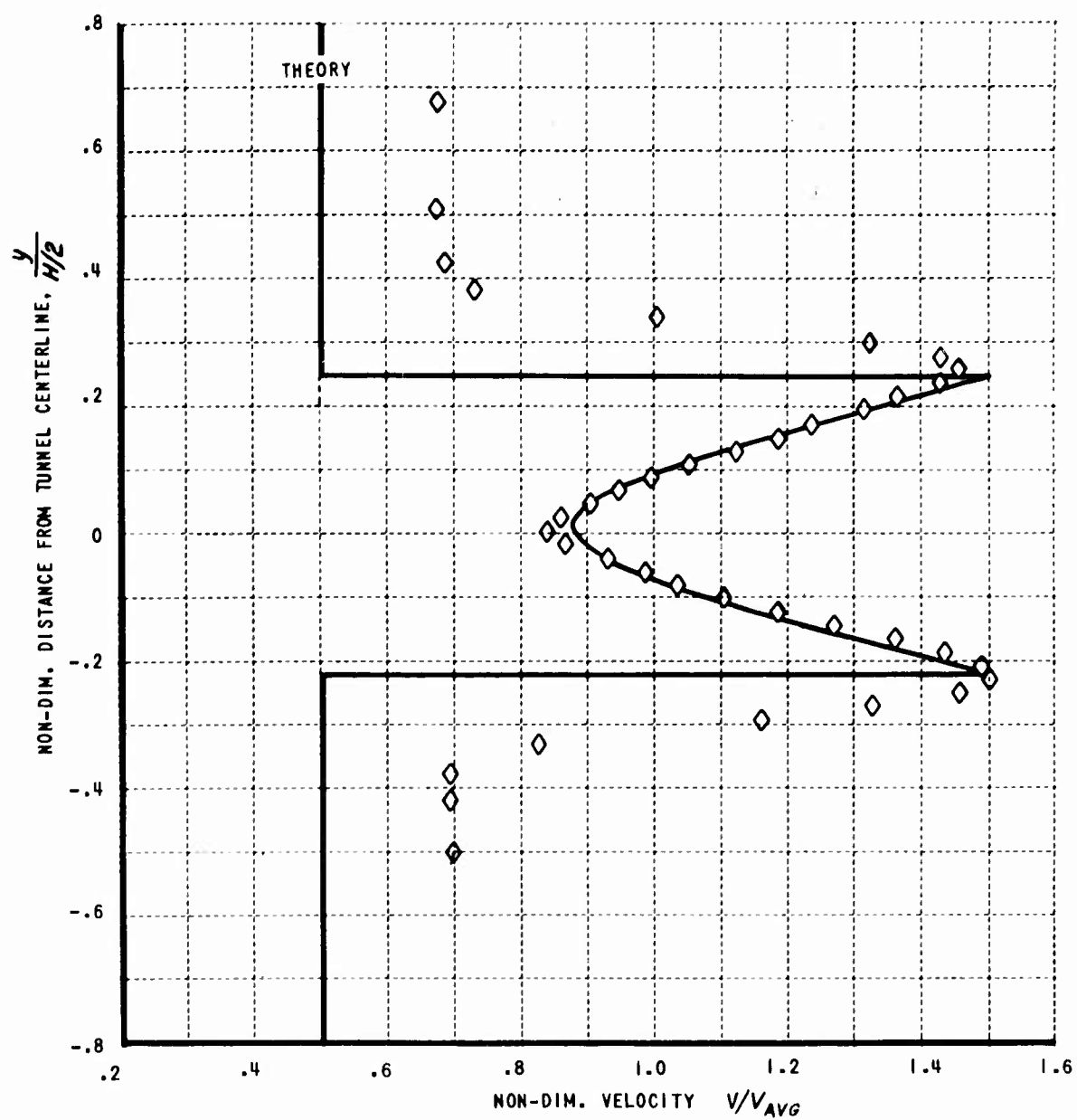
Figure 3C   VELOCITY DISTRIBUTION STA. B
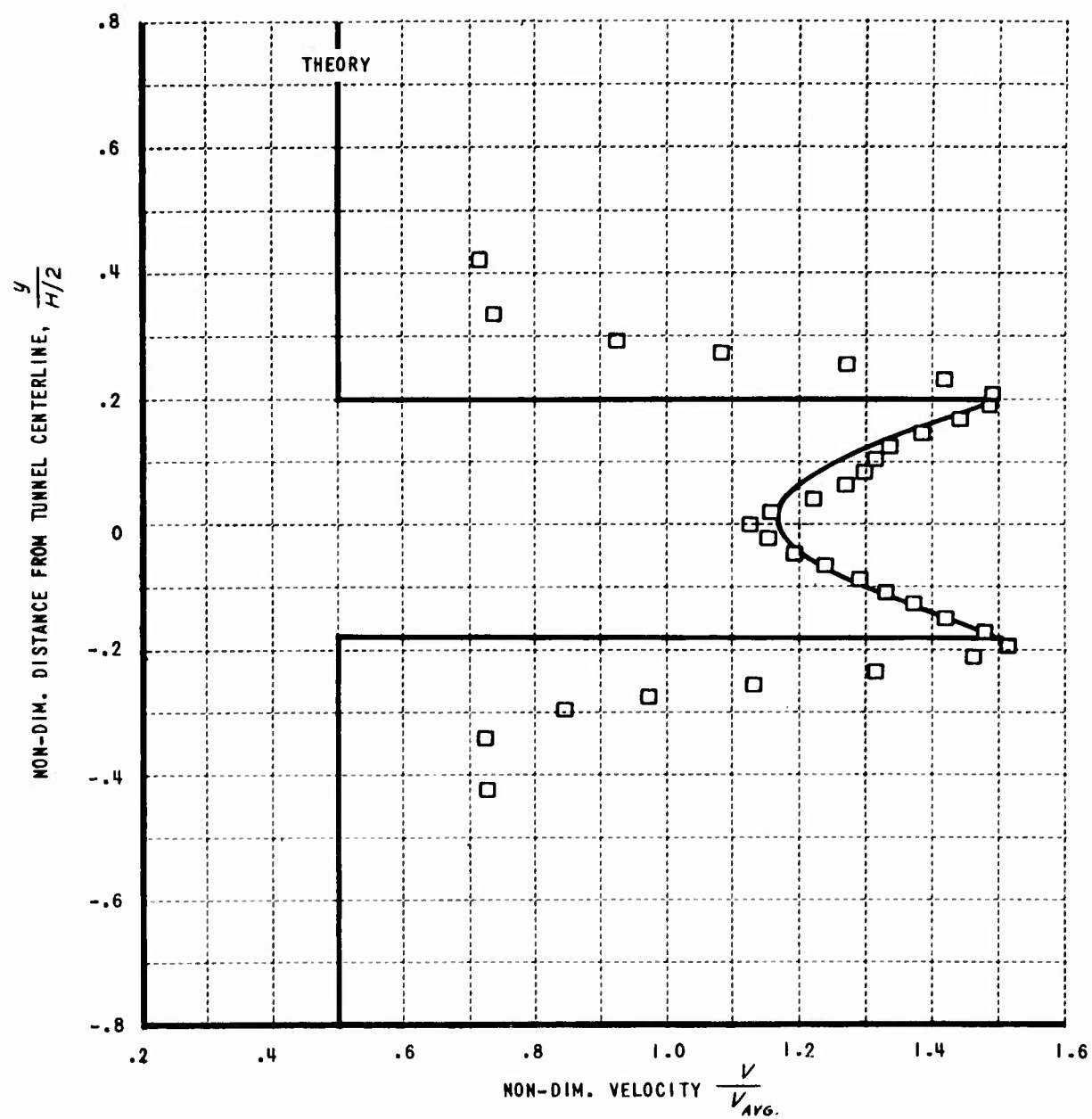
Figure 3D   VELOCITY DISTRIBUTION STA. C

30
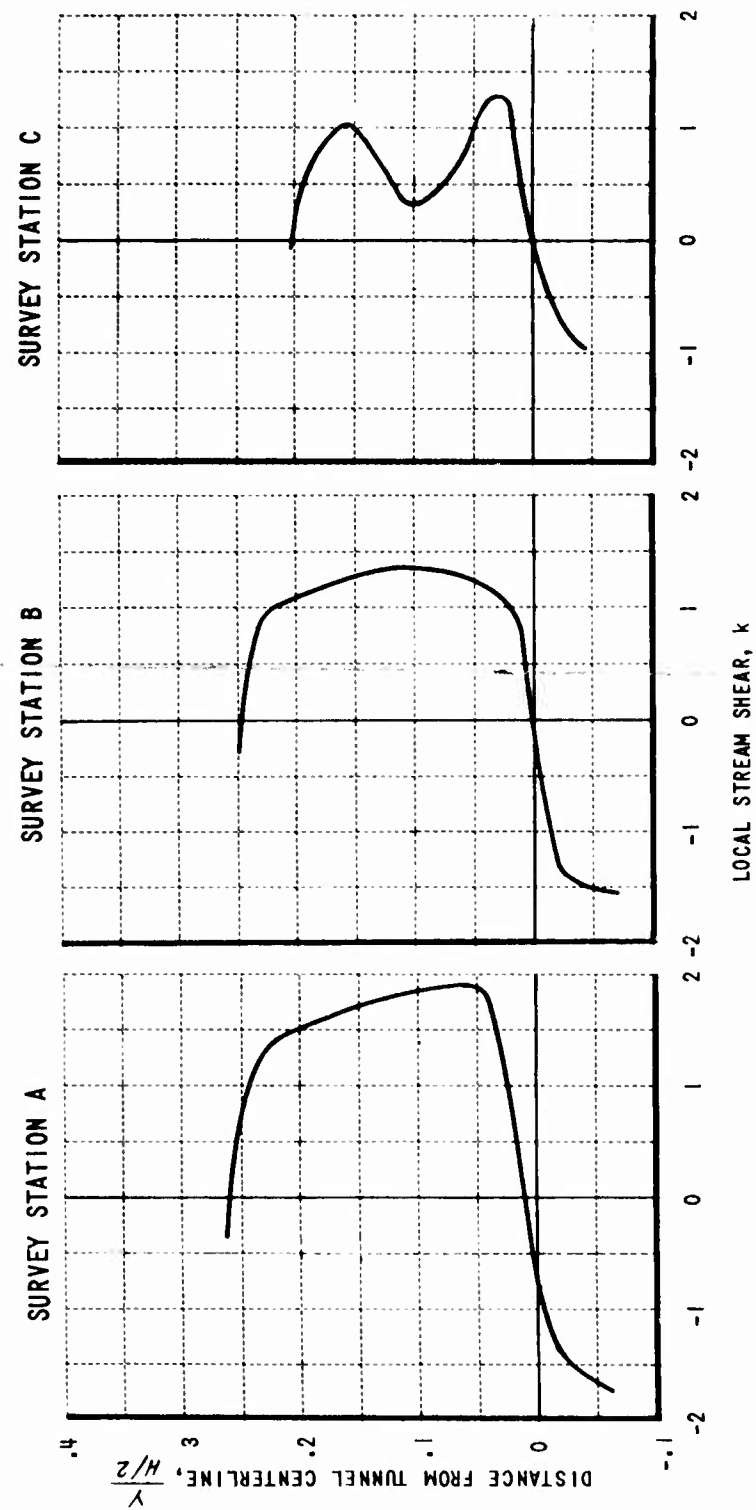
Figure 4 SHEAR DISTRIBUTION IN THE AXISYMMETRIC SLIPSTREAM

31
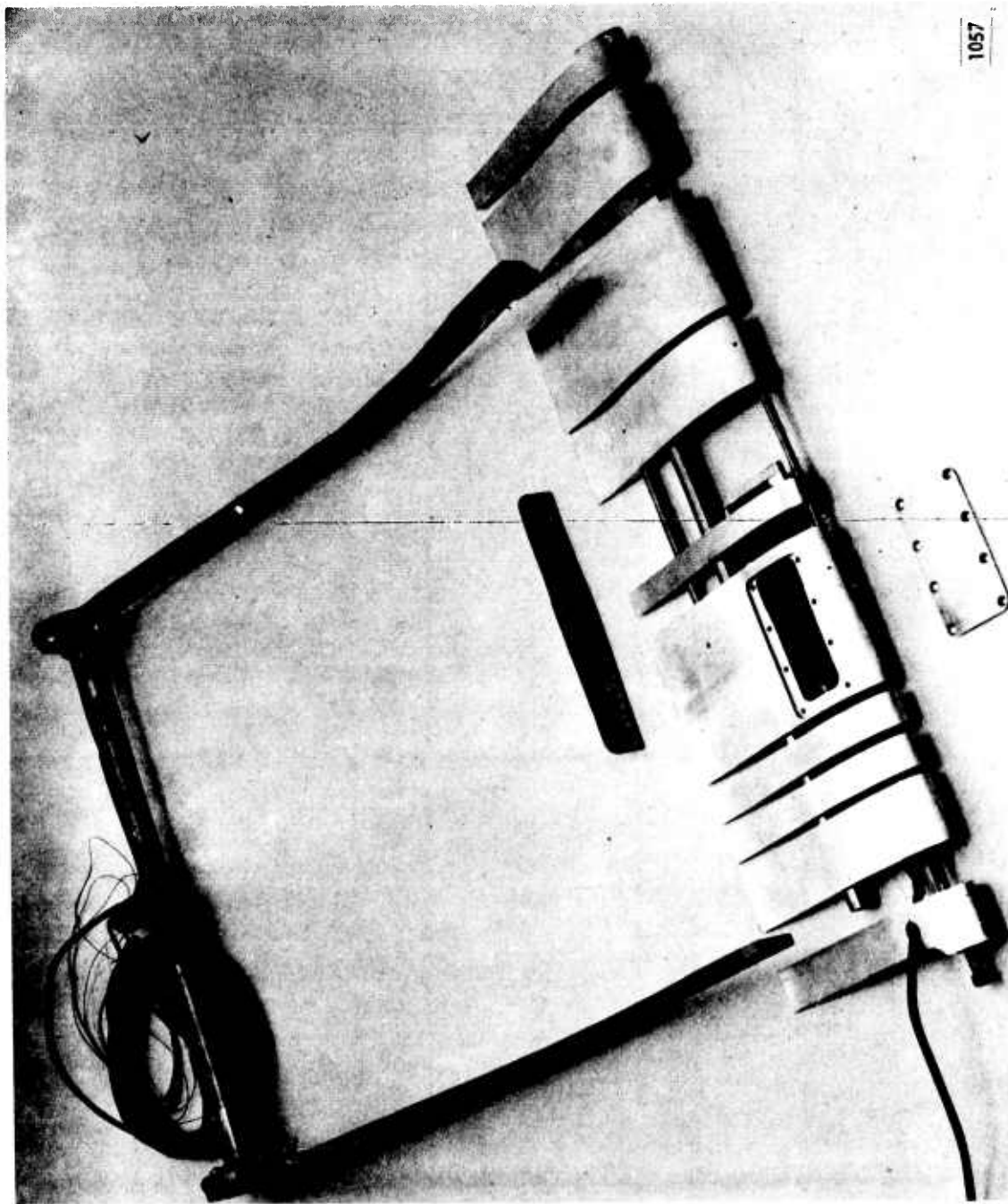
Figure 5   THE TWO-DIMENSIONAL SECTION LOAD MODEL

1057
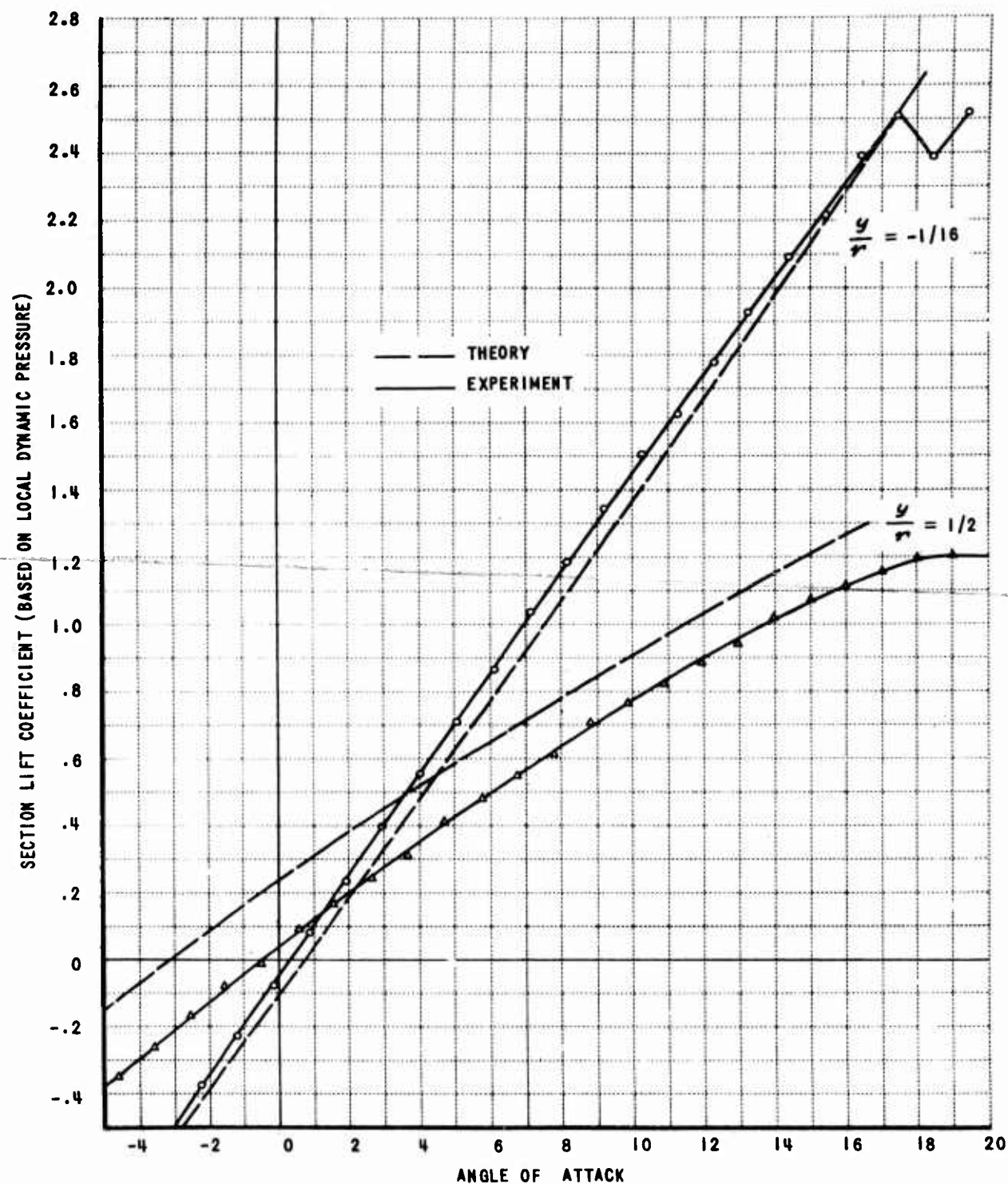
Figure 6   AIRFOIL SECTION LIFT IN THE
AXISYMMETRIC SLIPSTREAM

33
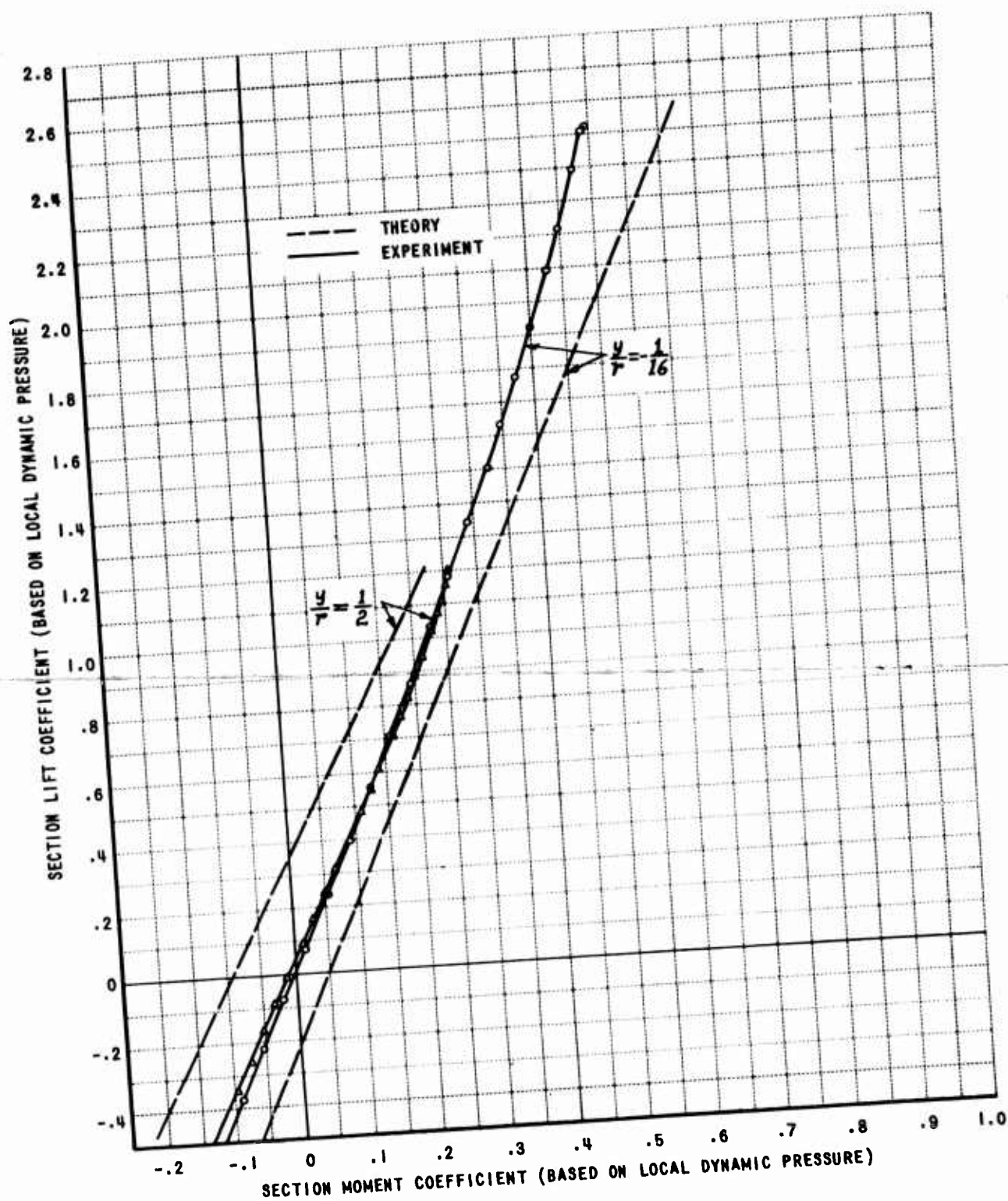
Figure 7 AIRFOIL SECTION PITCHING MOMENT
IN THE AXISYMMETRIC SLIPSTREAM

34
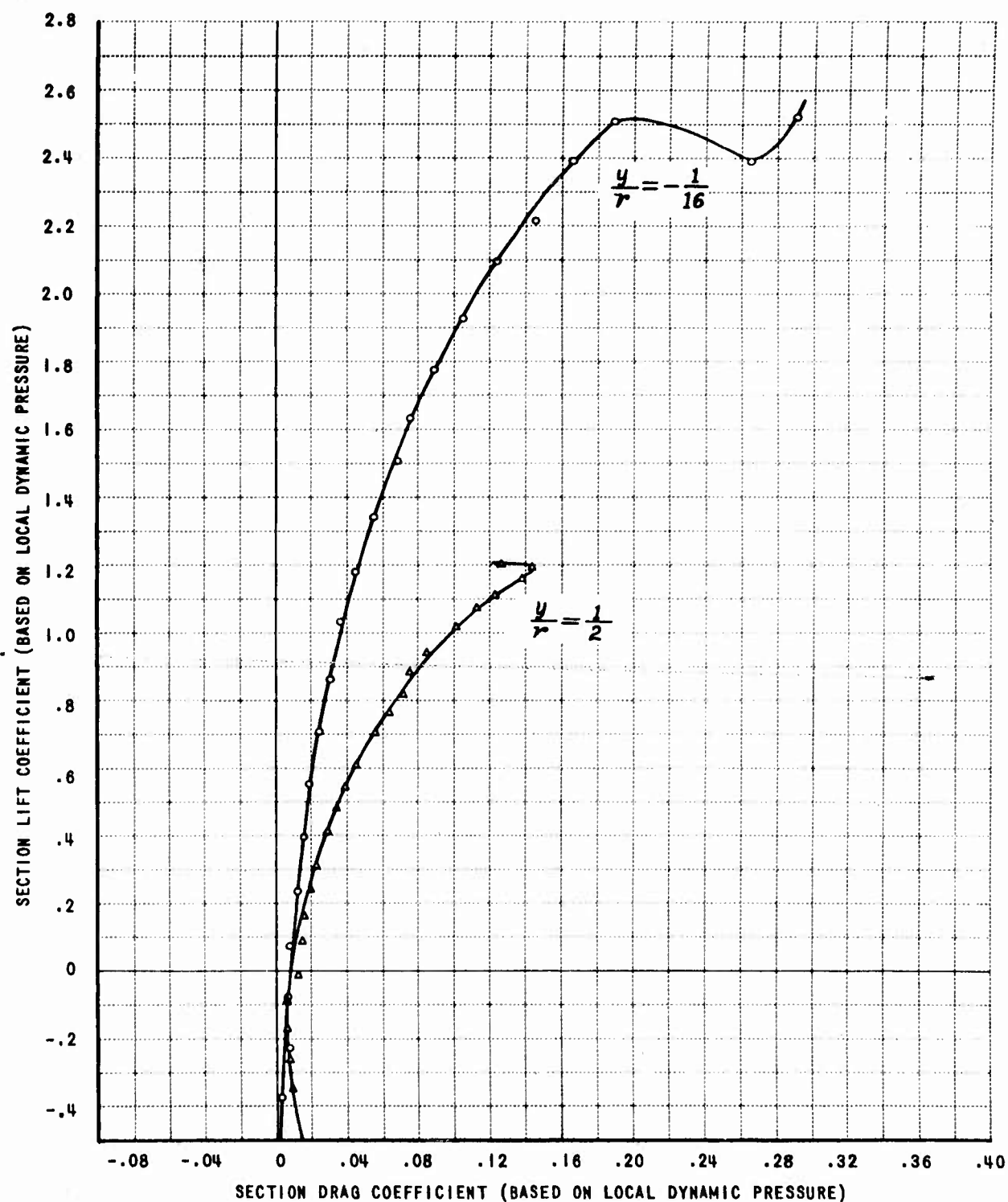
Figure 8   AIRFOIL SECTION DRAG IN THE AXISYMMETRIC SLIPSTREAM
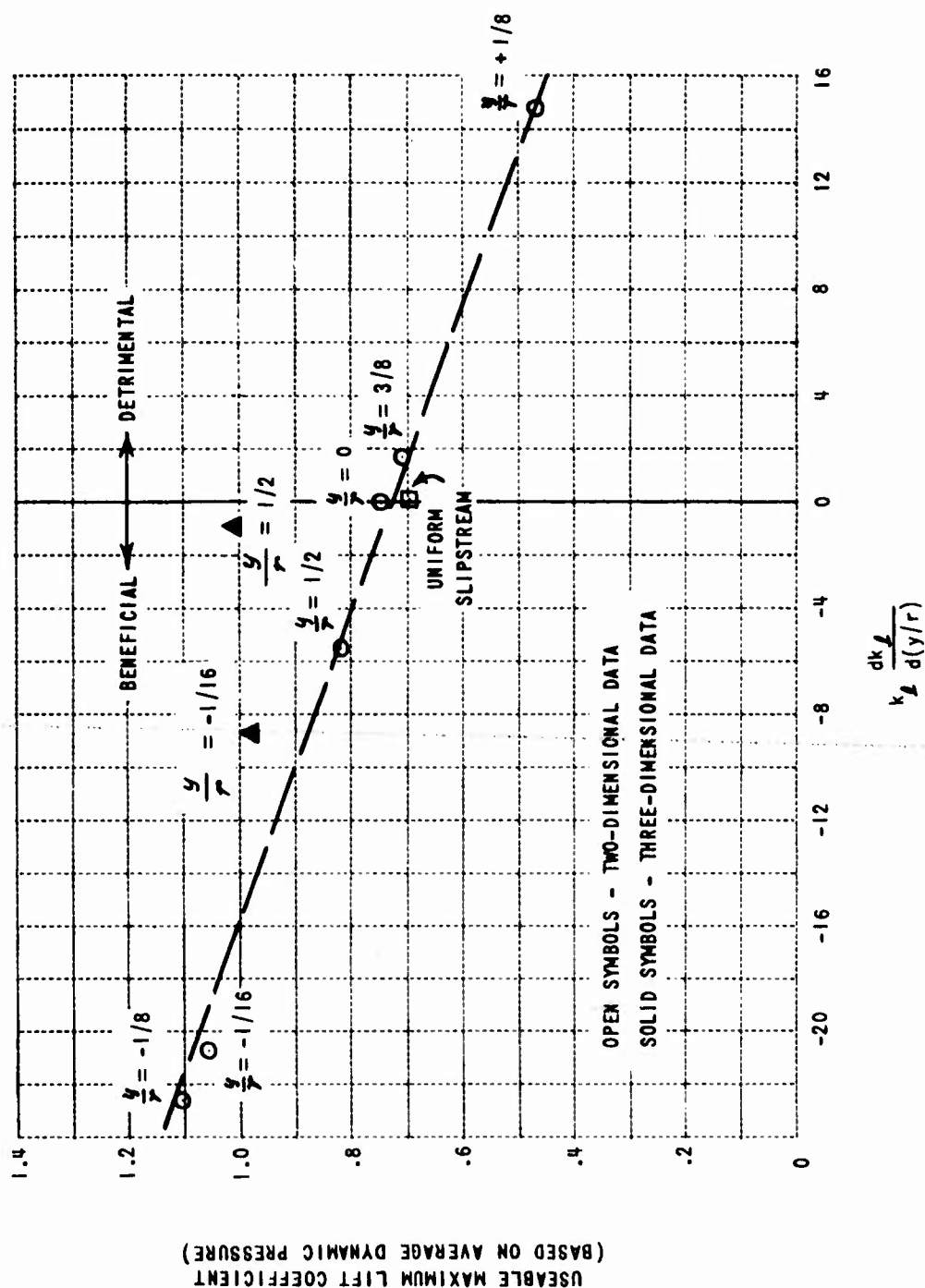
Figure 9 CORRELATION OF SECTION MAXIMUM LIFT WITH STREAM PROPERTIES
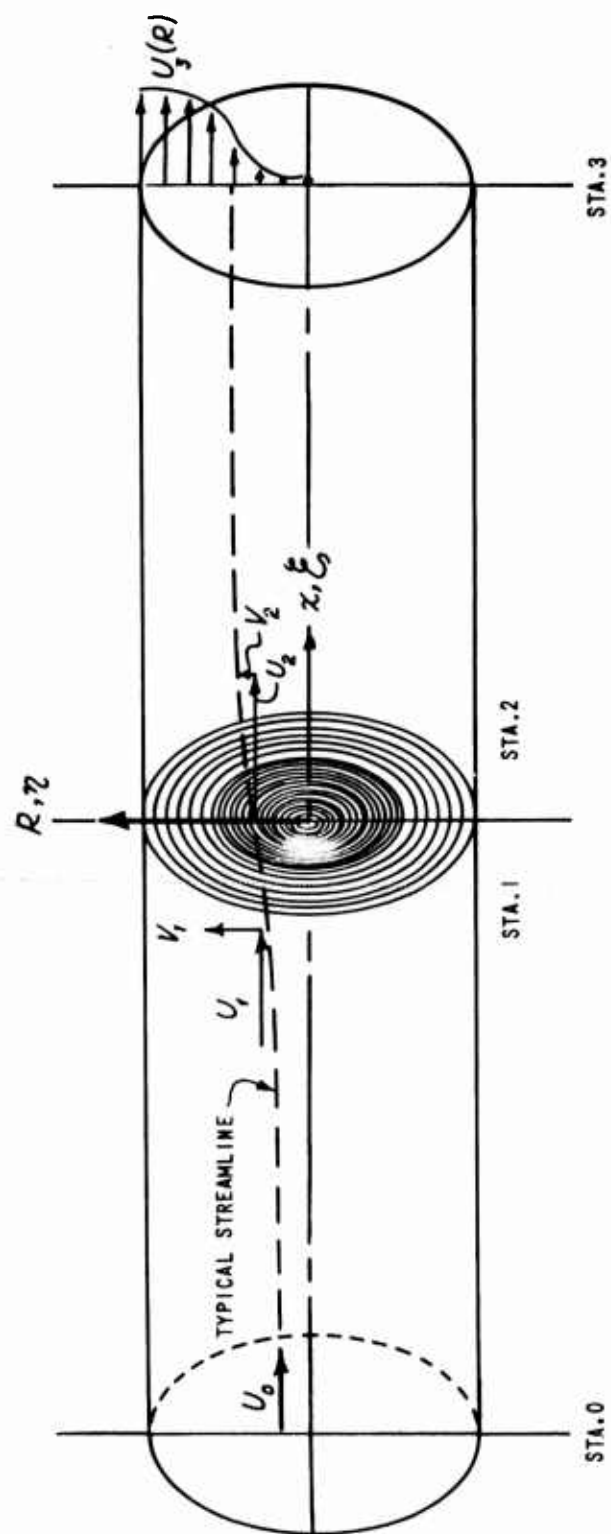
Figure 10 MODEL OF AXISYMMETRIC CHANNEL FLOW THROUGH A SCREEN

37

DISTRIBUTION LIST

Chief of Transportation, DA	(3)
USA Transportation Research Command	(27)
USA Transportation Materiel Command	(19)
Air Research & Development Command	(1)
Office of Chief of R&D, DA	(1)
Air Force Systems Command	(1)
Chief of Naval Research	(1)
NASA, Washington, D. C.	(4)
Langley Research Center, NASA	(1)
Ames Research Center, NASA	(1)
Lewis Research Center, NASA	(1)
Armed Services Technical Information Agency	(10)
USATRECOM Liaison Officer, USA R&D Liaison Group (9851 DU)	(1)
Canadian Army Liaison Officer, USA Transportation School	(3)
British Joint Services Mission (Army Staff)	(3)
U.S. Army Standardization Group, Canada	(1)
U.S. Army Standardization Group, U. K.	(1)
Institute of the Aerospace Sciences	(1)
USATRECOM Liaison Officer, USA Engineer Waterways Experiment Station	(1)
USATRECOM Liaison Officer, U.S. Army Aviation School	(1)

39

TC Liaison Officer, USA ERDL	(1)
USATRECOM Liaison Officer, Detroit Arsenal	(1)
USATRECOM Liaison Officer, Airborne and Electronics Board	(1)
USATRECOM Liaison Office, Wright-Patterson AFB	(1)
Bell Aerosystems Company	(1)
Bell Helicopter Company	(1)
The Boeing Company	(1)
Cornell University, Ithica, N. Y.	(1)
Cornell University, Buffalo, N. Y.	(25)
Fairchild Aircraft Division	(1)
General Electric Company	(1)
Goodyear Aircraft Corporation	(1)
Grumman Aircraft Engineering Corporation	(1)
Hiller Aircraft Corporation	(1)
Kaman Aircraft Corporation	(1)
Lockheed Aircraft Corporation	(2)
McDonnel Aircraft Corporation	(1)
Piasecki Aircraft Corporation	(1)
Republic Aviation Corporation	(1)
Ryan Aeronautical Company	(1)
General Dynamics Corporation	(1)
United Aircraft Corporation	(1)

AD-

Cornell Aeronautical Laboratory, Inc., Buffalo, New York

THE EFFECTS OF AXISYMMETRIC SHEAR ON AIRFOIL CHARACTERISTICS - R. J. Vidal, and J. T. Curtis.

CAL Report No. AI-1190-A-8, December 1961, 25 pp. - illus. (Contract No. DA 44-177-TC-439) Task 9R 38-11-009-03

Exploratory experiments with a two-dimensional airfoil in a simulated axisymmetric slipstream are described. The data are compared with the available theory and experimental data for two-dimensional flows to determine the effects of axisymmetric shear on airfoil characteristics. It is concluded that the two-dimensional results can be applied in a strip analysis near the axis of symmetry to determine lift curve slope and center of pressure. However, the two-dimensional results are not adequate for predicting the lift increment to shear and the influence of shear on airfoil maximum lift.

AD-

Cornell Aeronautical Laboratory, Inc., Buffalo, New York

THE EFFECTS OF AXISYMMETRIC SHEAR ON AIRFOIL
CHARACTERISTICS - R. J. Vidal, and J. T. Curtis.

CAL Report No. AI-1190-A-8, December 1961, 25 pp. - illus.
(Contract No. DA 44-177-TC-439) Task 9R 38-11-009-03

Exploratory experiments with a two-dimensional airfoil in a
simulated axisymmetric slipstream are described. The data
are compared with the available theory and experimental data
for two-dimensional flows to determine the effects of axisym-
metric shear on airfoil characteristics. It is concluded that
the two-dimensional results can be applied in a strip analysis
near the axis of symmetry to determine lift curve slope and
center of pressure. However, the two-dimensional results
are not adequate for predicting the lift increment to shear and
the influence of shear on airfoil maximum lift.

AD-

Cornell Aeronautical Laboratory, Inc., Buffalo, New York

THE EFFECTS OF AXISYMMETRIC SHEAR ON AIRFOIL
CHARACTERISTICS - R. J. Vidal, and J. T. Curtis.

CAL Report No. AI-1190-A-8, December 1961, 25 pp. - illus.
(Contract No. DA 44-177-TC-439) Task 9R 38-11-009-03

Exploratory experiments with a two-dimensional airfoil in a
simulated axisymmetric slipstream are described. The data
are compared with the available theory and experimental data
for two-dimensional flows to determine the effects of axisym-
metric shear on airfoil characteristics. It is concluded that
the two-dimensional results can be applied in a strip analysis
near the axis of symmetry to determine lift curve slope and
center of pressure. However, the two-dimensional results
are not adequate for predicting the lift increment to shear and
the influence of shear on airfoil maximum lift.